Authors' accepted manuscript
Article published in Canadian Journal of Civil Engineering, 2025.
The final published version available at https://doi.org/10.1139/cjce-2025-0093

MULTI-SCALE ANALYSIS OF THE IMPACT OF GRAPHENE OXIDE IN CEMENT-BASED MATERIALS

Victor Brial[a*], Claudiane Ouellet-Plamondon[a], Thomas Duplessis[a]

[a] Département de Génie de la construction, École de technologie supérieure, 1100 Notre-Dame Ouest, Montréal, Québec, Canada H3C 1K3

*Corresponding author:*victor.brial@etsmtl.ca;*

Abstract

This study investigates the effects of 0.03% graphene oxide (GO) on cement-based materials, focusing on dispersion methods (superplasticizers and sonication), water-to-binder ratios (0.35 and 0.4), and binary binders with 30% slag or 8% silica fume. Isothermal calorimetry revealed that well-dispersed GO enhances hydration reactions, notably the C_3A peak, through its nanofiller effect. Compressive strength tests showed that GO reduces fresh mortar flow but improves strength when combined with superplasticizers, emphasizing their role in achieving GO's potential. Chloride penetration tests at 28, 56, and 91 days demonstrated that GO reduces chloride ingress by 5.5%–24.9%, particularly in slag concretes, with lower W/B ratios further improving resistance. The addition of 8% silica fume significantly enhanced durability due to its fine particle size. These results suggest that properly dispersed GO, especially with superplasticizers, can improve both durability and mechanical properties of cementitious materials, offering practical benefits for construction applications.

Keywords:
Graphene oxide, supplementary cementitious materials, calorimetry, Rapid Chloride Penetration Test, mortar, concrete, durability

1- Introduction

Reducing CO_2 emissions related to cement consumption remains a significant challenge in the construction industry. Optimizing concrete mix design and using efficient grades of concrete where applicable can reduce material consumption and, consequently, CO_2 emissions (Scrivener, John et Gartner, 2018). Achieving durable and high-performance concrete often necessitates using high-range water reducing admixtures (HRWA) and supplementary cementitious materials (SCM) in the mix design (Nkinamubanzi, Mantellato et Flatt, 2016).

Recent advances in nanomodified cementitious composites, particularly using graphene oxide (GO), have shown promise in enhancing concrete performance. Studies reveal that incorporating a small percentage of GO into cement paste, mortar, and concrete significantly improves compressive, flexural, and tensile strength, as well as corrosion resistance (Chuah *et al.*, 2014 ; Bhojaraju *et al.*, 2021 ; Devi et Khan, 2020). This improvement is attributed to GO's nucleation effect on C-S-H crystal growth, akin to the filler effect, where materials provide favorable surfaces for C-S-H nucleation (Lv *et al.*, 2013 ; Lv *et al.*, 2014 ; Meng *et al.*, 2021 ; Lothenbach, Scrivener et Hooton, 2011 ; Kumar *et al.*, 2017). GO's hydrophilic nature, derived from its functional groups (hydroxyl, epoxy, carboxyl), facilitates its dispersion in water (Chuah *et al.*, 2014 ; Mohammed, Al-Saadi et Sanjayan, 2018 ; Wang *et al.*, 2020).

GO also influences the morphology of hydration products. Studies indicate that GO addition promotes the formation of hydrate agglomerations, yielding flower-like structures that contribute to strength enhancement (Lv *et al.*, 2013 ; Lv *et al.*, 2014). However, Cui et al. suggest these structures might be calcium carbonate artifacts from sample preparation (Cui *et al.*, 2017). Beyond morphology, Zhao et al. hypothesize that GO integrates into C-S-H structures, filling gel pores and densifying the cement paste microstructure (Zhao *et al.*, 2018).

Despite these findings, Yang et al. argue that GO does not alter C-S-H's microstructure but accelerates hydration, enhancing mechanical properties (Yang *et al.*, 2017). The pore

structure also benefits, with reduced porosity and finer gel pores observed in GO-modified mixes, especially at lower water-to-binder ratios (Lv *et al.*, 2014 ; Gong *et al.*, 2015). Thermogravimetric analysis (TGA) confirms increased bound water and calcium hydroxide content with GO addition, consistent with enhanced hydration rates (Gong *et al.*, 2015). Isothermal calorimetry further demonstrates GO's role in accelerating hydration and intensifying reaction peaks (Lu *et al.*, 2017).

However, not all studies report positive effects. Krystek et al. observed an 11% decrease in compressive strength in GO-modified mortars due to poor workability (Krystek *et al.*, 2019). The interaction of GO with blended cements is less explored, though recent findings suggest improved fluidity and mechanical properties in nano-modified slag-based binders (Bhojaraju *et al.*, 2021).

Proper dispersion of GO is critical to achieving its benefits, as its interaction with Ca^{2+} ions can lead to agglomeration, compromising performance (Liu *et al.*, 2020 ; Zhao *et al.*, 2020) (Zhao *et al.*, 2020). Dispersion methods such as superplasticizers, which form protective barriers around GO, and sonication, are commonly employed, though they vary significantly between studies (Bhojaraju *et al.*, 2021 ; Meng *et al.*, 2021 ; Liu *et al.*, 2020 ; Liu *et al.*, 2021). Given the improved microstructure with GO, its potential impact on durability is noteworthy, particularly in addressing chloride penetration and carbonation, which cause steel corrosion in reinforced concrete (Mirsayapov, Yakupov et Hassoun, 2020). However, durability studies on GO-modified concrete remain limited.

The objectives of this research are to evaluate the impact of adding a small percentage of graphene oxide (GO) on the performance and durability of concrete and cementitious materials. The study focuses on the behavior of GO with Portland GU cement, as well as its effect in combination with a binary binder mix with silica fume and slag. Additionally, the importance of nanoparticle dispersion is investigated through different sample preparation techniques.

To achieve these objectives, a multi-scale experimental program was designed and executed in three stages. The first stage aimed to understand the microstructure and hydration process of cementitious pastes incorporating GO. This involved analyzing the effects of superplasticizers, GO dispersion, binder type, and water-to-binder ratio. Isothermal calorimetry was conducted on various mixes to evaluate the impact of GO on binder hydration.

The second stage focused on mechanical properties, specifically compressive strength and workability. These tests adhered to the CSA A3004 C-2 standard, with variables such as binder type, superplasticizer use, and GO dispersion systematically manipulated. Flow measurements were also performed to assess the influence of GO on fresh-state properties.

The third stage evaluated the practical applicability of GO-modified concrete. Concrete mixes were designed to meet Canadian standards. Comparisons were made between GO-modified and conventional mixes through compressive strength and chloride ion penetration tests conducted at 28, 56, and 91 days. Additionally, fresh-state characterizations, including density, slump, and air content, were performed to assess the consistency and workability of the mixes.

While numerous studies have demonstrated the potential of graphene oxide (GO) in enhancing cementitious materials, most have focused on paste-level or small-scale mortar investigations under idealized laboratory conditions. This study extends the current knowledge by evaluating GO's influence across multiple scales—pastes, mortars, and structural concretes from realistic Canadian standard constraints (e.g., CSA, Ministère des transports et de la mobilité durable (MTMD) du Québec). It compares two practical dispersion methods (superplasticizer vs. sonication), explores hybrid binders with slag and silica fume, and includes durability testing via RCPT. These aspects are typically overlooked in previous studies, especially the link between GO dispersion quality, SCM synergy, and performance at different W/B ratios at the structural concrete level.

2. Materials and methods

2.1 Materials

In this research, the binders used in for the different steps of the research program consisted of a general use Portland cement (GU), granulated ground blast furnace slag (GGBS), and silica fume (SF). Table 1 presents the chemical analysis of the binders. Particle size distribution of the binders, presented in Figure 1, was also determined by laser granulometry. Graphene oxide consisted of a commercially available graphene oxide water dispersion at a 0.4 wt% concentration. Figure 2 shows a flake of GO observed with a transmission electron microscope (TEM). Table 2 presents the elemental analysis for the commercially available GO.

For mortars, ASTM C778 natural silica graded sand was used. For concrete mixes, two types of coarse aggregates were used, a 5-20 mm limestone and 5-14 mm granitic aggregates. Both aggregates respected the CSA specifications for particle size distribution (CSA group, 2019). Natural sand was used as the fine aggregates. Particle size distribution and the fineness modulus of sand also respected the Canadian standards. To meet the required slump and air content in concrete mixes, two types of polycarboxylate superplasticizer and air entraining admix were used.

2.2 Sample preparation and testing

2.2.1 GO sonication

Sonication of GO-water solutions was performed for some mixes. The 0.04% graphene oxide dispersion was added to the amount of water needed to make each of the paste and mortar mixes. The beaker filled with GO dispersion was then installed in the protective box and the instrument probe lowered into the solution. The cavitation resulting from the sonication allows the separation of the agglomerates from the particles leading to a more uniform dispersion of the nanoparticles. A Qsonca brand and model Q700 device

programmed at an amplitude of 30 for 15 minutes was used to disperse the nanoparticles. Mixes with sonicated GO are represented with the “+” symbol.

2.2.2 Isothermal calorimetry

For the calorimetry tests, the ASTM C1702 standard " Standard Test Method for Measurement of Heat of Hydration of Hydraulic Cementitious Materials Using Isothermal Conduction Calorimetry " was followed. This standard consists in determining the heat of hydration of a cement paste by comparing the results obtained for the different binders with an inert reference sample. Raw materials were mixed by hand for one minute directly in the ampoule, the duration of the test was 7 days and the test temperature was 23°C. The tested mixes are presented in Table 3. Among the 36 mixes, the variables manipulated were the W/C ratio, the addition of GO, the addition of blast furnace slag, the use of superplasticizer and the sonication of the GO solution. The pastes were mixed by hand directly into the ampoule using a glass rod.

2.2.3 Mortar tests

For the mortar compression tests, mixes were made in accordance with the material proportions prescribed in CSA A3004-C2: Test Method for Determining Compressive Strengths. For each of the mixes, twelve mortar cubes of 50 mm × 50 mm × 50 mm were made. For each mix, 3 cubes were tested for compressive strength, at 1, 3- and 28-day intervals. A MATEST hydraulic press programmed with a 2000 kN cell and a loading rate of 1 kN/s was used to determine the compressive strength of the mortar specimens. Table 4 shows the different mixes and the proportions of materials used for the tests. The reference samples consist of GU cement mortar with and without superplasticizer. The same mixes were then reproduced, this time adding graphene oxide equivalent to 0.03% of the total mass of the binder. The same series of cubes was replicated with a ternary binder of GU and slag. A total of 18 mixes were made to understand the effect of GO on GU cement and blended cement, as well as the method of GO dispersion on the mechanical strength of the mortars. According to Shang *et al.* (2015), GO significantly influences the rheology of cementitious materials by increasing both yield stress and viscosity. Therefore,

to remain consistent with the CSA A3004-C2 standard for compressive strength testing, the dosage of superplasticizer was adjusted to maintain a constant mortar flow of 110 ± 5%.

2.2.4 Concrete tests

For this part, superplasticizer was used as the only dispersion method. It should be considered that the amount of GO solution to be dispersed for concrete manufacturing was much higher than those for pastes and mortars (359 ml for mortars versus 7 liters for concrete). Sonication of such a volume would not have been possible with the sonicator used in this research.

Concrete must often meet prescriptive standards and performance requirements to be used as safe and durable construction materials. For this research, the concrete mix designs are based on Quebec Ministry of Transportation type V-S and XIII mixes and CSA A23.1 type C-1 and C-XL mixes. Table 5 shows the target characteristics for the concrete mixes. The mixes based on the requirements of type V-S/C-1 concretes were made with the 5–20 mm limestone aggregate. The mass of binder used is 390 kg/m³ and the water/binder ratio is 0.4. The dosage of admixes was adjusted during the batch to achieve the desired slump and air content. For this category of mixes, different binders were used. First, reference mixes were made. These mixes consisted of concrete made with GU cement and GUb-30S blended cement. To evaluate the combination of graphene oxide with these two types of binders, the same mixes were then made by adding 0.03% of GO of the total binder mass. Finally, a reference mix meeting MTMD requirements was fabricated with a GUb-S/SF binder type. This mix will be used as a reference to evaluate the performance of graphene oxide concrete compared to concrete typically used for the construction of civil engineering structures. Such concretes are commonly used in transportation infrastructure, including bridge decks, abutments, and highway barriers, where high durability against freeze–thaw cycles and chloride ingress is essential.

In order to evaluate the behavior of GO on mixes with a higher binder content and a lower W/B ratio, the concrete was designed with a composition meeting both the specifications

of the Quebec Transport Ministry (MTMD, Ministère des Transports) and the Canadian Standard Association (CSA) (Table 5). For this experiment, aggregate of granitic nature and size 5-14 mm was chosen. The binder mass used is 450 kg/m^3 and the W/B ratio is set at 0.35. The admixture dosage varies from one concrete to another in order to obtain the desired slump. For theses mix designs, the types of binders are the same as those previously mentioned. Thus, 5 formulations inspired by a type V-S/C-1 concrete and 5 formulations inspired by a type XIII/C-XL concrete have been made.

The concrete mixes were manufactured in accordance with CSA Standard A23.2-2C (CSA group, 2019). GO dispersion was mixed water and SP and added in the mixer during the mixing process. Slump tests, air content tests and density determination were also performed on the fresh concrete. A total of 22 concrete cylinders were made for each of the different mixes. The CSA A23.2-3C test method: making and curing concrete compression and flexural test specimens was followed for the manufacture of the 100 mm diameter and 200 mm long cylinders. The specimens were then unmolded at 23h ± 1h and placed in a 100% humidity chamber.

Rapid chloride penetration testing was done accordingly to the ASTM 1202-19 Standard Test Method for Electrical Indication of Concrete’s Ability to Resist Chloride Ion Penetration tests (RCPT) (ASTM International, 2019). For each mix, three 50 mm samples, sawed from the concrete cylinders, were tested at 28, 56 and 91 days. A RCPT testing device made by Germann Instrument was used for testing the specimens. The initial measurement of the current and every 30 minutes was recorded for 6 hours. The values are plotted on a current (amperes) versus time (seconds) graph. The integral of the area under the curve corresponds to the load in Coulomb (ampere-seconds). RCPT results can give a qualitative indication of the chloride ion penetrability of concrete. The smaller the coulomb value, the better the material's resistance to chloride ion penetration. Although the Rapid Chloride Migration Test (RCMT) may offer greater accuracy for evaluating chloride diffusivity, particularly in SCM-rich systems, the Rapid Chloride Permeability Test (RCPT) was chosen in this study to comply with Canadian (CSA A23.2-23C) and Quebec

(MTMD 3102) testing standards. This approach also ensures direct comparability with commonly accepted performance thresholds used in industry.

3. Results and analysis

The results of the multi-scale analysis on cement pastes, mortars and concretes are presented in the following sections.

3.1 Isothermal calorimetry

To facilitate the presentation of the results and to better understand the impact of GO on binder hydration, the 36 curves were separated by binder type and W/B ratio. Thus, four graphs for heat flow in mW/g and four graphs for cumulative heat of hydration in J/g are drawn. For the heat flow graphs, the x-axis was also reduced to 60 hr to better obtain a better resolution of the different peaks. Figure 3a and Figure 3b show the GU type mixes with a W/B ratio of 0.4. First, as expected, the use of superplasticizer in the mix delays the setting of the cement by about 3.5 hours. These results agree with the literature regarding the effect of polycarboxylate superplasticizers on cement setting. This delay in the reaction would be the result of chelation formed in the paste between the Ca^{2+} ions and the admixture. This interaction would help reduce the Ca^{2+} concentration, preventing nucleation of solid phases and hydration of reaction products, leading to a delay in the reaction (Zhang *et al.*, 2010).

For the samples without superplasticizer, the addition of graphene oxide and graphene oxide dispersed by sonication does not appear to convincingly affect the peak heat of hydration, as the intensity and position of the silicate and aluminate peaks remain comparable to those of the control mixture. When combined with superplasticizer, the GU 0.4 SP GO+ blend appears to show a larger peak than the GU 0.4 SP blend, with a value of 3.21 mW/g versus 3.07 mW/g, respectively. The second hydration peak, which corresponds to the hydration of C_3As, is amplified and more distinguishable by the addition of GO and superplasticizer. For the cumulative heat graph in Figure 3b, it is observed that the addition of superplasticizer to the GU 0.4 SP, GU 0.4 SP-GO, and GU 0.4 SP-GO+

mixes delays the heat gain of hydration. From 28 hours to 38 hours of hydration, all mixes appear to have released the same amount of heat. Beyond 38 hours, the heat released by the mixes with graphene oxide and superplasticizer exceeds that of all other mixes. The mix with GO sonication (GU 0.4 SP-GO+) shows the highest cumulative heat after 160 hours.

For GU cement samples with a W/B ratio of 0.35, the same trends as for the previous mixes are observed. As shown in Figure 4a, the addition of superplasticizer shifts the curves to the right, with GU 0.35 SP being the most delayed and the SP-GO and SP-GO+ peaks appearing to be slightly superior to SP alone. In addition, the C_3A hydration peaks for the GU 0.35 SP-GO and GU 0.35 SP-GO+ blends are amplified. The second hydration peak, for these mixes, however, is more intense than for the curves of the pastes with higher W/B ratio. Again, as with the 0.4 mixes, the cumulative heat curves in Figure 4b, show that the addition of superplasticizer to the GU 0.35 SP, GU 0.35 SP-GO, and GU 0.35 SP-GO+ mixes delays the heat gain of hydration. At about 32 hours, these same mixes begin to exceed the mixes without admixes in terms of total heat.

Mixes with a binary binder composed of 30% slag are presented in Figure 5 and 6. Essentially the same observations are made as for the GU mixes. The addition of superplasticizer shifts the maximum to the right, the C_3A peak is amplified for mixes with SP and GO and the lower the W/B ratio the larger the second maximum. Also, for samples with SP, those with GO+ show a moderately higher peak than the mix with only SP. There does not appear to be any visible synergy or interaction between GO and slag that significantly affects the shape of the curves.

Figure 7a illustrates the heat flow of GUb-SF mixes with a water-to-binder (W/B) ratio of 0.4. The addition of superplasticizer (SP) delays the setting time of the cement, shifting the heat flow peak to the right, though this delay is less pronounced compared to other samples tested. Interestingly, the sample without SP shows a slightly higher heat peak of silicate (C_3S) compared to the samples with SP. The inclusion of graphene oxide (GO) and graphene oxide dispersed by sonication (GO+) in mixes containing SP results in higher

peak heat flow compared to the mix with SP alone. The amplified C_3S and C_3A hydration peaks in the SP-GO and SP-GO+ mixes suggest enhanced hydration activity due to the presence of GO, which may improve dispersion and interaction with cement particles. For the cumulative heat release for these mixes is depicted. The presence of SP initially delays the cumulative heat gain, consistent with its known retardation effect. The total heat released varies differently depending on the mixes. For mixes without GO and with GO dispersed by sonication, the total heat slightly decreases with the addition of SP. However, for mixes with GO alone, the total heat increases with the addition of SP. After the initial delay, the mixes containing SP, SP-GO, and SP-GO+ surpass the cumulative heat release of the mix without SP. Among these, the mix with GO+ exhibits the highest cumulative heat after an extended period, indicating that the enhanced dispersion of GO through sonication contributes to prolonged and efficient hydration, resulting in greater total heat release over time.

Figure 8a presents the heat flow of GUb-SF mixes with a W/B ratio of 0.35. As observed in Figure 7a, the addition of SP delays the peak heat flow, though the delay is less significant compared to other samples tested. However, the peak heights are very similar across all mixes, with no distinct effects of C_3S or C_3A hydration visible. The lower W/B ratio results in more intense and faster hydration peaks compared to the higher W/B ratio mixes, indicating accelerated hydration kinetics. Figure 8b shows the cumulative heat release for these mixes. The addition of SP causes an initial delay in cumulative heat gain, consistent with its retardation effect like observed for the other samples. Despite the presence of SP, GO, or sonication, the total cumulative heat release for all samples tested is very similar, indicating that these additives do not significantly affect the total heat released. This suggests that the presence of SP, GO, or GO+ does not result in major differences in overall hydration efficiency for this W/B ratio.

Discussion on isothermal calorimetry results

For calorimetry tests, the effect of GO and GO dispersion method was studied on GU cement and GU blended cement paste made with 30% GGBFS. W/B ratios of 0.4 and 0.35 were also used. As observed previously, it turns out that the type of binder, the W/B ratio

and the use of superplasticizer are the parameters that have a greater impact on the shape of the heat release rate (mW/g) and cumulative heat of hydration (J/g) curves. The theoretical influence resulting from the manipulation of these variables was observed in the graphs. The effect of GO was more subtle, hence the need to separate the curves by binder type and by W/B ratio. The effect of GO, that the rate of cement dissolution is increased, setting is accelerated, heat of hydration is increased and C_3A hydration is affected, can to some extent be seen in the results. It was first observed that the height of the heat rate peak could be slightly increased by the addition of GO+, especially for the mixes with SP, where the same observations were seen in all four graphs. However, this conclusion cannot be validated for mixes without SP.

The most notable feature of the addition of GO is the shape of the calcium aluminate hydration peak, which is amplified by the addition of graphene oxide. This phenomenon is observed on binary binder pastes and GU cement pastes and is more prominent when GO is dispersed with superplasticizer. It is also more pronounced in mixes with lower W/B ratio, where the amount of GO per volume of paste is higher. This occurrence can be attributed to the level of undersaturation of C_3A and gypsum resulting from the introduction of GO into the mix. The functional groups of the GO reacting with Ca^{2+} allow the Ca^{2+} concentration in the porous solution to be reduced, thereby facilitating the dissolution of the C_3As (Kang *et al.*, 2020). Drawing a parallel with the filler effect, another possible explanation could explain these results. Indeed, similarities can be drawn between the results obtained and some studies conducted on the use of quartz and limestone powder as filler and on the filler effect of supplementary cementitious materials. The acceleration of the aluminate peak associated with the use of these fillers is associated with the nucleation effect and the specific surface area of these materials, which contribute to accelerating and amplifying the hydration of the cement components (Zunino et Scrivener, 2019). Therefore, it is possible that C_3A peaks are affected by the nanofiller effect of GO. The heat released after 160 h was also used to perform a factorial ANOVA according to the factors and levels shown in Table 6. The results of the ANOVA and the main effects plot are available in figure 9 and Table 7.

The heat released by cement paste, measured by isothermal calorimetry, reveals significant findings across several factors. The binder demonstrates a strong effect on the heat released, indicated by a high F value and an extremely low p-value. The binder type significantly influences the heat released, as visually confirmed in the main effect plot where the mean heat values differ noticeably among the binder types (GU, GUb-S, and GUb-SF), with GU showing the highest mean heat and GUb-SF the lowest.

The water-to-binder ratio (W/B) also exhibits a substantial impact on the heat released, evidenced by a very high F value and an extremely low p-value. The main effect plot supports this finding, showing a clear increasing trend in mean heat values as the W/B ratio increases from 0.35 to 0.40. This indicates that higher water-to-binder ratios are associated with increased heat release in the cement paste. The presence of a superplasticizer significantly affects the heat released, as reflected by a moderate F value and a low p-value. The main effect plot shows a slight increase in mean heat values when a superplasticizer is used compared to when it is not, indicating that superplasticizers enhance the heat release of the cement paste.

In contrast, the GO does not significantly influence the heat released, as indicated by a low F value and a high p-value. The main effect plot shows little variation in mean heat values across the different levels of graphene oxide treatment (No, Yes GO, Sonication GO+), suggesting that the addition of graphene oxide, regardless of the method of incorporation, does not significantly affect the heat release in the cement paste. Overall, binder type and W/B ratio are the most critical factors influencing the heat release in cement paste, while the superplasticizer has a moderate effect and graphene oxide has a negligible impact.

3.2 Mortar compressive strength

The results of flow and compressive strength tests at 1, 7 and 28, for mixes with GU are presented in Figure 10. The black curve corresponds to the flow percentage. First, the addition of 0.03% GO to the mortar significantly reduces the flowability of the mix from 69% to 49%. This decrease in workability resulting from the use of GO is well documented in the literature. For mortar mixes, the flow required by the standard is 105 ± 5% (CSA,

2018). To approach the specified flow, the addition of superplasticizer to the GU mix is required. The superplasticizer used as a dispersant in the GO solution also contributed to a better flow for the mortar, but still being insufficient to meet the 105 ± 5%. At 1 day, the GU+GO mix gives a strength of 7.1 MPa against 8.4 MPa for the reference mix. This is a decrease of 16%.

When dispersed with superplasticizer, the strength of the mortar with GO, in young age, is, however, higher than the control, 10.5 MPa against 8.4 MPa, for an increase of 24%. However, this increase in strength must be attributed to the use of the superplasticizer and not to the GO, since the strength of the GU-SP mix is 10.30 MPa. When dispersed with the sonicator, the GO does not appear to contribute further to the strength development of mortars. At 1 day, the mix with the highest strength remains the GU-SP. At 7 days, the trends remain the same as those observed at 1 day, except for the GU-SP-GO+ mix which shows the highest strength, 38.4 MPa versus 36.6 MPa for GU-SP. However, performing a statistical test does not confirm that the GU-SP-GO+ mix is better than GU-SP. Indeed, the null hypothesis that the mean of the two samples is equal is confirmed. At 7 days, it can also be seen that the difference between the mixes with superplasticizer and without superplasticizer is larger. For example, the difference at 1 day between GU and GU SP is 22%, while at 7 days this difference is 36%. Finally, at 28 days, there is no significant change with respect to the observations presented for the 1 day and 7 days time frames. The mortars that provide the best compressive strength are those with superplasticizer, particularly GU-SP and GU-SP-GO+, with 46.2 and 46.8 MPa. The addition of GO alone significantly reduces the strength.

For mixes shown in Figure 11, with 30% of slag, the flow percentage results are slightly higher than for the GU mortar. The fluidizing aspect of slag due to the glassy particles of this SCM is well apparent with the results obtained with the flow table test (De Belie, Soutsos et Gruyaert, 2018). As expected, workability is reduced by the addition of 0.03% GO, but can be compensated by the addition of superplasticizer. As observed with GU mortars, the addition of GO does not contribute to improving the compressive strength properties of the mortar. Rather, the increase in strength is attributed to the use of

superplasticizer. At 1 day, the GUb-S SP mix is the strongest with 7.7 MPa, followed by the GUb-S-SP-GO with 7.4 MPa. At 7 days, GUb-S-SP-GO with 34.2 MPa shows the highest strength. Again, the 28-day results follow the same trends as the other time frames. Mixes with superplasticizers continue to perform best. The addition of GO alone is detrimental to the strength gain of the mortar and GO+ and GO dispersed with SP do not show any advantage over the GUb-SP mix.

For the mixes shown in Figure 12, which incorporate silica fume (SF), the compressive strength results are significantly influenced by the presence of superplasticizer (SP) and graphene oxide (GO). At 1 day, the GUb-SF-SP mix shows the highest compressive strength, highlighting the positive impact of superplasticizer in the early curing phase. This mix achieves a compressive strength close to 20 MPa, indicating rapid strength development facilitated by the superplasticizer. The GUb-SF-GO mix, on the other hand, demonstrates a lower compressive strength, around 10 MPa, suggesting that the addition of GO alone does not contribute positively to early strength gain. The mix GUb-SF-SP-GO, which combines both superplasticizer and GO, shows improved performance compared to the GO-only mix, but it does not surpass the strength of the GUb-SF-SP mix.

At 7 days, the trend observed at 1 day continues. The GUb-SF-SP mix still exhibits the highest compressive strength, reaching approximately 40 MPa. This result reinforces the effectiveness of the superplasticizer in enhancing the strength of the mortar. The GUb-SF-GO mix shows a modest increase in strength compared to its 1-day performance but remains lower than the superplasticized mixes. The GUb-SF-SP-GO mix shows an improvement, indicating that the combination of superplasticizer and GO can enhance strength development, albeit not as effectively as superplasticizer alone.

By 28 days, all mixes show significant increases in compressive strength. The GUb-SF-SP mix achieves the highest strength, nearing 55 MPa, followed closely by the GUb-SF-SP-GO mix. This suggests that while GO can contribute to long-term strength gain when used with superplasticizer, it is not as effective as superplasticizer alone. The GUb-SF-GO mix, despite showing improvement over time, remains the lowest in compressive strength

among the tested mixes, indicating that GO alone is not sufficient for optimal strength development. These results demonstrate that the addition of superplasticizer significantly enhances the compressive strength of silica fume mortars across all curing periods. The inclusion of graphene oxide does not independently improve compressive strength and may require the presence of superplasticizer to be effective. These findings suggest that for the best performance in terms of compressive strength, the use of superplasticizer is essential, while the addition of graphene oxide should be carefully considered.

Discussion on compressive strength results

As expected, the addition of GO to mortar mixes greatly reduces the workability of mixes with and without superplasticizer. The large specific surface area of the graphene oxide particles affects the water demand and therefore reduces the workability. In terms of compressive strength, the addition of GO and GO+ to the mixes without superplasticizer significantly reduced the compressive strength of the cubes. These results are consistent with some data available in the literature, where the compressive strength of a GU cement mortar is reduced by the addition of GO (Krystek *et al.*, 2019). This decrease in strength may be associated with the poor workability of the fresh mix that did not allow for good compaction of the mortar and good dispersion and reactivity of the cement particles. A visual inspection of the hardened mortars of GU-GO+ allowed to observe a significant number of voids, which could explain the reduction in strength.

As for the mixes, where GO and GO+ were dispersed with superplasticizer, a beneficial effect on the compressive strength was expected. However, the strength gain is instead attributed to the use of superplasticizer and not to the addition of graphene oxide. The addition of SP to the mix with GO results in values similar to the control mix. The compressive strength data at 1 day and 28 days were also used to perform a factorial ANOVA according to the factors and levels shown in Table 8. The results of the ANOVA and the main effect plots are available in Figures 13 and 14, as well as Tables 9 and 10, respectively.

Compressive strength of mortar at one day indicates significant effects for the binder and the superplasticizer, while the graphene oxide does not appear to have a statistically significant impact. The binder has the most substantial effect on the compressive strength, as indicated by its high F value and extremely low p-value. This suggests that changes in the type of binder used have a marked impact on the strength of the mortar at the one-day mark. The main effect plot for the binder shows that the GU binder results in a moderate means compressive strength, whereas the GUb-S binder yields a lower strength. The GUb-SF binder shows a significant increase, achieving the highest compressive strength among the binders tested.

For the superplasticizer, the results also show a significant effect, with an F value indicating a meaningful impact and a p-value that is below the threshold for significance. This implies that the inclusion of a superplasticizer positively influences the mortar's compressive strength at one day. The main effect plot supports this finding, as the presence of a superplasticizer results in higher mean compressive strength compared to when it is absent.

In contrast, the graphene oxide factor does not exhibit a statistically significant effect on the compressive strength. The results show a relatively low F value and a p-value that is well above the typical significance level, indicating that variations in the levels of graphene oxide (including no graphene oxide, graphene oxide with sonication, and graphene oxide without sonication) do not significantly alter the compressive strength. The main effect plot for graphene oxide levels illustrates this lack of significant variation, with mean compressive strength values remaining relatively consistent across the different levels. In summary, the type of binder and the use of a superplasticizer are crucial factors that significantly affect the one-day compressive strength of mortar. In contrast, the inclusion and variation of graphene oxide do not have a meaningful impact within the parameters of this study. The graphical representations corroborate these findings, showing distinct differences in mean compressive strengths associated with binder types and the presence of a superplasticizer, while the graphene oxide levels exhibit minimal variation.

Compressive strength of mortar at 28 days reveals significant effects of all three factors: binder type, superplasticizer use, and graphene oxide inclusion. The F values and p-values indicate that each factor contributes notably to variations in compressive strength. Starting with the binder type, the analysis shows that this factor has a significant impact on compressive strength. The graphical representation indicates an increasing trend in the mean strength as we move from GU to GUb-S and finally to GUb-SF. This suggests that the combination of GUb-S and GUb-SF provides a notable enhancement in the mortar's compressive strength compared to the GU binder. The use of superplasticizer shows an even more pronounced effect. The presence of superplasticizer significantly increases compressive strength. The mean strength is substantially higher when superplasticizer is used, as depicted in the main effects plot. This indicates that superplasticizers play a crucial role in enhancing the performance of the mortar by improving its workability and subsequent strength.

Graphene oxide's influence is also significant, with a measurable impact on compressive strength. The main effect plot for graphene oxide shows a nonlinear trend: the mean strength initially decreases when GO is added without sonication but increases again when GO is dispersed using sonication. This pattern highlights the importance of dispersion quality, as sonication appears to improve the distribution of GO within the cement matrix, leading to better particle interaction and enhanced strength. Although no benefit was observed at 1 day, the increased compressive strength at 28 days suggests that the positive effects of sonicated GO become more prominent over time due to improved nucleation sites and microstructural refinement. The main effect plots further show that among the three studied factors—binder type, superplasticizer, and graphene oxide—the binder type and superplasticizer have the strongest influence, with steep changes in average strength across levels, while GO presents a more modest but statistically significant contribution. These plots are particularly valuable because they isolate the effect of each variable on compressive strength while averaging out the influence of the others. This statistical approach helps identify which factors drive performance and supports decision-making in mix design. These findings are especially relevant in the context of structural concrete, where achieving optimal mechanical performance is essential. The results underline the

potential of carefully adjusted multi-component mixes, where superplasticizer use and GO dispersion method can be leveraged to fine-tune strength development.

3.3 **Concrete compressive strength and chloride penetration resistance**

Table 11 shows the fresh concrete properties and 28-day compressive strength for each of the mixes. These tests are used to verify the compliance of the mixes with the Quebec MTMD Standard 3102. As mentioned previously, these tests are intended to evaluate the compliance of the mixes with the requirements specified in the standards for concrete used in civil engineer constructions. RCPT results are only considered in this paper for discussion and analysis. Except for the GU 0.4 and Type V-S GUb-S/SF, where the air content is above the standard limit, the slump, air content and compressive strength requirements are met for the samples. It was not considered necessary to rework the batches of non-compliant concretes, given the low impact of entrained air on the resistance to chloride ion penetration.

The results of the 28-, 56-, and 91-day chloride ion penetration tests for mixes based on V-S concrete (W/B ratio of 0.4) are shown in Figure 15. The red line on the graph corresponds to the 1000-coulomb limit required, at 56 days, by the MTMD standard, while the blue line is the 1500 limit required by the CSA standard, at 91 days. The error bars consist of the confidence interval calculated from a 95% confidence index.

It is first observed that for all mixes, the coulomb value is reduced, the older the concrete, which means a better resistance to chloride penetration from the early age to 91 days. Secondly, it is apparent that the addition of supplementary cementitious materials (SCMs) to the concrete mixes significantly reduces the coulomb value of the samples. For this series of mixes, the addition of GO to GU cement concrete does not appear to improve the chloride ion resistance properties. It is also possible to state that concrete with GU as the sole binder is far from being able to meet the 1000-coulomb requirement specified by the standard. Mixing with 30% slag considerably reduces the penetration of chloride ions. This decrease is on average 38.8% compared to the GU mix. Although the GU-GO mix does not improve the performance of the concrete, the addition of GO to the blended binder seems to slightly reduce the chloride ion penetration. This reduction averages 7.4%

compared to the GUb-S mix and 47.7% compared to the GU 0.4 mix. Finally, the typical V-S mix with silica fume is greatly superior to the other 4, with an average decrease of 86% compared to the GU mix. It is also the only mix that meets MTMD requirements, with a value of 307 coulombs at 56 days. However, for the 1500 coulombs limit of the CSA standard, GUb-30S and GUb-30S-GO concretes meet the requirements. The results for the mixes with a higher amount of cement and a W/B ratio of 0.35 are shown in Figure 16. The red line consists of the 1000-coulomb limit prescribed by the CSA and MTMD standard.

As expected, as the concrete ages, the chloride ion penetration value decreases. In addition, as previously observed, the addition of supplementary cementitious materials also improves the performance of the concrete. However, in contrast to the previous mixes, the addition of GO to concrete with a higher Portland cement content and a lower W/B ratio seems to improve the properties. A decrease in coulombs of 21.6%; 5.5% and 8.2% is observed at 28, 56 and 91 days, respectively. At 28 days, this decrease is more noticeable and statistically significant. For the 56- and 91-day maturities, it is not possible to state that the addition of GO improves the chloride ion penetration resistance of General Use cement concrete.

Compared to the GUb-30s mix, the GUb30s-GO mix shows a decrease in chloride ion penetration of 24.9%; 17.8% and 14.3% at 28, 56 and 91 days, respectively. This decrease is 55.3%, 46.5% and 43.5% compared to the reference mix. Again, the decrease is most striking at 28 days. The effect of GO on resistance to chloride ion penetration appears to be more pronounced on mixes with a higher cement content and lower W/B ratio. Like the 0.4 W/B mixes, the concrete with silica fume shows the best performance in the RCPT test. It is also the only mix that meets the 1000-coulomb requirement established by the department of transportation.

Discussion on RCPT results

First, the wide confidence intervals can be explained by the small number of samples and the poor reproducibility of the test. The standard specifies that the coefficient of variation can reach 12.3% for the same mix tested by the same operator (34% variation for the same

samples). Secondly, the results showed that the factors that most influenced the performance of the material against chloride ion penetration were the curing period of the concrete and the choice of a binder type. More advanced hydration and a more refined pore structure explain these results. In addition, supplementary cementitious materials, which are smaller in size than cement particles, subdivide the pore structure of the concrete, thereby reducing permeability (Stanish, Hooton et Thomas, 1997). Laser diffraction analysis of binders clearly shows the difference in particle sizes of cement, slag and silica fume.

For the GO modified samples, 3 concretes showed a slight decrease in coulombs compared to their reference, GUb-S GO 0.4 at 91 days, GU 0.35-GO at 28 days and GUb-S 0.35 GO for all time frame. Based on the information gathered in the literature review, this improvement could be attributed to the refined pore structure resulting from the addition of GO. Indeed, the pore structure has a significant impact on the chloride ion penetration value (Stanish, Hooton et Thomas, 1997) and GO can contribute to modifying the porosity as well as the pore size of a cement paste (Lv *et al.,* 2013). The effect of GO in mixes inspired by Type XIII concretes is more convincing than in Type V-S mixes, since both concretes (GU-GO and GUb-S) showed a significant difference with their controls. Considering that the dosage of GO is done in relation to the mass of cement, there will necessarily be more GO nanoparticles in the total mix (0.03% of 450kg/m3 versus 0.03% of 390 kg/m3). Moreover, for the same volume, the number of GO nanoparticles will be greater in a 0.35 W/B paste than in a 0.4 W/B paste. The effect of GO is more pronounced in mixes with a high quantity of cement and a low W/B ratio. A parallel can be made with the calorimetry results, where the C3A hydration peak for SP-GO mixes is more intense with a W/B ratio of 0.35 than for a W/B ratio of 0.4. The results of the type XIII mixes also showed that the difference between the GO-modified mixes and the standard was more pronounced at 28 days. Following the theory that graphene oxide acts as a nucleation site for cement hydration, allowing for greater C-S-H crystallization during the first few days of curing, it is possible that this observation is related to this explanation. Since the cement continues to hydrate slowly over time, the reference mixes appear to catch up to the concretes with GO at 56 and 91 days. While it appears advantageous to use GO and a

combination of slag and GO to reduce chloride ion penetration, in a practical context, the use of GO is far from sufficient to meet the chloride ion penetration requirements specified by the standards. Typical mixes, XIII and V-S with slag and silica fume are far superior to GO modified mixes.

4. Discussion

The results of the multiscale analysis on the effectiveness of GO in GU and compound binder cementitious matrices were found to be mixed. On the one hand, the calorimetry tests showed results consistent with the literature. Regardless of binder type and W/B ratio, the impact of superplasticizer-dispersed GO was seen in the height and position of the heat flow peaks and in the intensity of the C_3A peaks. Comparing the filler mechanism with the results obtained, it is plausible to think that the nucleation effect is responsible for these observations.

On a larger scale, the results of the compressive strength tests on mortar did not give the expected results. Without superplasticizer, a significant decrease in strength was even noted. The effect of GO on the workability of the mortar can easily explain these results. However, when combined with superplasticizer and dispersed properly, it would have been expected to obtain higher strength values than the controls. Sonication of the GO solution did not appear to show a significant impact on the results.

Finally, little research had been done on the resistance to chloride ion penetration of GO modified concrete. The results obtained showed that GO could contribute to reducing the penetration of chloride ions, and that this reduction was more significant for mixes with a lower W/B ratio and a higher quantity of cement. The improvement of concrete properties by the addition of GO can possibly be explained by the refinement of the pore network resulting from the nucleation of C-S-H on the GO particles. Mercury intrusion porosimetry (MIP) or absorption test tests could be performed to confirm this hypothesis.

The addition of 0.03% GO to concrete, an economical dosage for structure, is not sufficient to significantly improve resistance to chloride ion penetration. From a practical application perspective, the 1000-coulomb limit specified by the Quebec Ministry of Transport

679 standard is not achieved in mixes with GO. One potential reason is that GO remains a
680 relatively new material in cement science. Unlike supplementary cementitious materials
681 (SCMs), which benefit from decades of standardization, there are currently no established
682 benchmarks to verify GO quality or ensure reproducibility between laboratories. As
683 highlighted in the literature review, the effects of GO vary widely, in contrast to the more
684 consistent performance reported for materials like silica fume or slag. The variability in
685 manufacturing routes and source materials may influence the physical and chemical
686 properties of GO, thus impacting its performance in cementitious systems. In contrast, the
687 8% silica fume used in this study consists of ultra-fine particles in the nanometer range,
688 which are well-known for their strong pozzolanic reactivity and ability to refine pore
689 structure, leading to significantly improved durability performance.
690
691 The GO dosage selected, 0.03% by weight of cement, was based on economic
692 considerations and previously reported optimal dosages (Krystek, 2019 ; Gong *et al.*,
693 2015). While some studies have tested dosages up to 1.6%, these are often impractical for
694 large-scale implementation. For example, increasing the dosage to 0.06% or 0.09% might
695 yield more pronounced effects, but it would also exacerbate the workability loss and
696 critically raise material costs (e.g., $750 USD for 40 g at laboratory scale). Moreover,
697 practical deployment at higher dosages remains constrained by dispersion challenges,
698 including incompatibilities with some superplasticizers and destabilization in the presence
699 of cementitious ions. These technical and economic barriers suggest that future research
700 should explore both hybrid nano-additive systems and optimized dispersion protocols to
701 enhance performance while remaining scalable.
702
703 ## 5. Conclusion

704 In conclusion, the work carried out in this study was aimed at pursuing the research on the
705 use of graphene oxide in cement-based materials. This research was conducted from a
706 fundamental point of view but also from a practical approach, to evaluate if this type of
707 material can compete with the concretes currently used in the industry. Therefore, the
708 objective of the research was to evaluate the impact of adding a small percentage of
709 graphene oxide nanoparticles (0.03%) on the physical, chemical, and mechanical properties

of cementitious materials, with a particular focus on concrete performance against chloride penetration. In addition to studying the behavior of GO with general usage Portland cement alone, the effect of GO combined with a binary binder mix (GU and blast furnace slag), the method of GO dispersion and the influence of W/B ratio on GO performance was studied.

- The calorimetry results on pastes showed agreement with the literature, especially in the height and position of the heat release rate peaks and in the intensity of the C_3A peaks. The effect of GO was more pronounced on lower W/B mixes. By comparing the mechanism of the fillers to the results obtained, it is plausible to think that the nucleation effect responsible for these observations.
- On a larger scale, the results of the compressive strength tests on mortar did not give the expected results. Without superplasticizer, a significant decrease in strength was even noted. When combined with superplasticizer and dispersed properly, it would have been expected to obtain higher strength values than the controls.
- For the concrete tests, the results obtained showed that GO could contribute to reducing the penetration of chloride ions, and that this reduction was more significant for mixes with a lower W/B ratio and a higher amount of cement.
- Finally, issues with the stability of the graphene oxide dispersion were observed when certain types of superplasticizers were used. An additional consideration must be given when choosing the dispersion method and superplasticizer. Overall, the results confirm that structural concrete incorporating silica fume, without GO, successfully meets the performance requirements specified by current durability standards.

All in all, it is well documented that carbon-based nanomaterials are beneficial for several industries. To date, it is estimated that over 40 applications can benefit from this type of technology. One of the most important uses is in the field of plastics and composites, where physical, electrical and thermal properties can be greatly improved by the addition of a small percentage of graphene-based materials. Other areas such as the automotive industry,

batteries and 3D printing are also areas where graphene can be beneficial (Barkan, 2019). As for concrete and cementitious materials, the large number of articles on the subject shows that this field has not escaped the graphene hype. However, when silica fume is used as a supplementary cementitious material in concrete, the effect of GO is not significant on the chloride permeability.

The research related to the use of GO still deserves to be pursued. In fact, it would be relevant to conduct studies to develop a procedure for the preparation of GO-modified cementitious materials, to ensure that the effect of GO is observable and consistent from study to study. There are currently significant gaps in inter-laboratory reproducibility, as it was noted in the literature review that the percentage increase in compressive strength of GO-modified materials can vary from -11 to 77%. There should also be more research into the use of GO on a larger scale. Many studies have been done on cementitious pastes and mortars only. However, for a normal density concrete, the aggregates can occupy more than 70% of the volume of the materials. Graphene oxide must become more economical to use at the structural level.

Acknowledgments

The support from NSERC (RGPIN 2016-05011), Quebec Centre for Advanced Materials (CQMF-QCAM), and the Canada Research Chair on Sustainable multifunctional construction materials (CRC-2019-00074) is greatly acknowledged. The support of Alexys is also recognized.

7. Author contribution statement:

Conceptualization: C.O.P.

Data curation: V.B., C. O.P

Formal analysis: V.B.

Funding acquisition: C.O.P.

Investigation: V.B., T.D., C.O.P.

Methodology: V.B., C.O.P,

Project administration: C.O.P

Resources: C.O.P.

Software: V.B., C.O.P.

Supervision: C.O.P supervised V.B. and T.D.

Validation: V.B. Visualization: V.B.

Writing - original draft: V.B.

Writing - review & editing: V.B. and C.O.P.

8. Competing interests statement

The authors declare there are no competing interests.

9. Data availability statement

Data generated or analyzed during this study are available from the corresponding author upon reasonable request.

10. References

ASTM International. 2019. « C1202 - 19 Standard Test Method for Electrical Indication of Concrete's Ability to Resist Chloride Ion Penetration ». *ASTM Standard Book*. <https://doi.org/10.1520/C1202-19>.

Barkan, Terrance. 2019. « Graphene: the hype versus commercial reality ». *Nature Nanotechnology*, vol. 14, nº 10, p. 904-906. <https://doi.org/10.1038/s41565-019-0556-1>.

Bhojaraju, Chandrasekhar, Seyed Sina Mousavi, Victor Brial, Michael DiMare et Claudiane M. Ouellet-Plamondon. 2021. « Fresh and hardened properties of GGBS-contained cementitious composites using graphene and graphene oxide ». *Construction and Building Materials*, vol. 300, p. 123902. <https://doi.org/10.1016/j.conbuildmat.2021.123902>.

Chuah, Samuel, Zhu Pan, Jay G. Sanjayan, Chien Ming Wang et Wen Hui Duan. 2014. « Nano reinforced cement and concrete composites and new perspective from graphene oxide ». *Construction and Building Materials*, vol. 73, p. 113-124. <https://doi.org/10.1016/j.conbuildmat.2014.09.040>.

CSA. 2018. *A3000-18 Compendium des matériaux liants*.

CSA group. 2019. *A23.1:19/A23.2:19 - Concrete materials and methods of concrete construction/Test methods and standard practices for concrete*.

Cui, Hongzhi, Xiantong Yan, Luping Tang et Feng Xing. 2017. « Possible pitfall in sample preparation for SEM analysis - A discussion of the paper “Fabrication of polycarboxylate/graphene oxide nanosheet composites by copolymerization for reinforcing and toughening cement composites” by Lv et al. » *Cement and Concrete Composites*, vol. 77, p. 81-85. <https://doi.org/10.1016/j.cemconcomp.2016.12.007>.

De Belie, Nele, Marios Soutsos et Elke Gruyaert, éd. 2018. *Properties of Fresh and Hardened Concrete Containing Supplementary Cementitious Materials: State-of-the-Art Report of the RILEM Technical Committee 238-SCM, Working Group 4*. Coll. « RILEM State-of-the-Art Reports ». Cham : Springer International Publishing. <https://doi.org/10.1007/978-3-319-70606-1>. Consulté le 20 avril 2021.

Devi, S.C. et R.A. Khan. 2020. « Effect of graphene oxide on mechanical and durability performance of concrete ». *Journal of Building Engineering*, vol. 27, p. 101007. <https://doi.org/10.1016/j.jobe.2019.101007>.

Gong, Kai, Zhu Pan, Asghar H. Korayem, Ling Qiu, Dan Li, Frank Collins, Chien Ming Wang et Wen Hui Duan. 2015. « Reinforcing Effects of Graphene Oxide on Portland Cement Paste ». *Journal of Materials in Civil Engineering*, vol. 27, nº 2. <https://doi.org/10.1061/(ASCE)MT.1943-5533.0001125>. Consulté le 3 mai 2021.

Kang, Xiaojuan, Xiaohong Zhu, Jiaping Liu, Xin Shu, Yongbo Huang et Jueshi Qian. 2020. « Dissolution and precipitation behaviours of graphene oxide / tricalcium silicate composites ». *Composites Part B: Engineering*, vol. 186, p. 107800. <https://doi.org/10.1016/j.compositesb.2020.107800>.

Krystek, Małgorzata. 2019. « Mechanical properties of cement mortar with graphene oxide ». *Architecture, Civil Engineering, Environment*, vol. 12, nº 1, p. 91-96. <https://doi.org/10.21307/acee-2019-008>.

Krystek, Małgorzata, Dawid Pakulski, Violetta Patroniak, Marcin Górski, Leszek Szojda, Artur Ciesielski et Paolo Samorì. 2019. « High-Performance Graphene-Based Cementitious Composites ». *Adv. Sci.*, p. 12.

Kumar, Aditya, Tandre Oey, Gabriel Falzone, Jian Huang, Mathieu Bauchy, Magdalena Balonis, Narayanan Neithalath, Jeffrey Bullard et Gaurav Sant. 2017. « The filler effect: The influence of filler content and type on the hydration rate of tricalcium silicate ». *Journal of the American Ceramic Society*, vol. 100, nº 7, p. 3316-3328. <https://doi.org/10.1111/jace.14859>.

Liu, Changjiang, Xiaochuan Huang, Yu-You Wu, Xiaowei Deng, Zhoulian Zheng, Zhong Xu et David Hui. 2021. « Advance on the dispersion treatment of graphene oxide and the graphene oxide modified cement-based materials ». *Nanotechnology Reviews*, vol. 10, nº 1, p. 34-49. <https://doi.org/10.1515/ntrev-2021-0003>.

844 Liu, Lang, Jie Xin, Chongchong Qi, Hailiang Jia et KI-IL Song. 2020. « Experimental
845 investigation of mechanical, hydration, microstructure and electrical properties of
846 cemented paste backfill ». *Construction and Building Materials*, vol. 263, p.
847 120137. <https://doi.org/10.1016/j.conbuildmat.2020.120137>.

848 Lothenbach, Barbara, Karen Scrivener et R. D. Hooton. 2011. « Supplementary
849 cementitious materials ». *Cement and Concrete Research*, vol. 41, n° 12, p.
850 1244-1256. <https://doi.org/10.1016/j.cemconres.2010.12.001>.

851 Lu, Zeyu, Xiangyu Li, Asad Hanif, Binmeng Chen, Pavithra Parthasarathy, Jinguang Yu
852 et Zongjin Li. 2017. « Early-age interaction mechanism between the graphene
853 oxide and cement hydrates ». *Construction and Building Materials*, vol. 152, p.
854 232-239. <https://doi.org/10.1016/j.conbuildmat.2017.06.176>.

855 Lv, Shenghua, Jingjing Liu, Ting Sun, Yujuan Ma et Qingfang Zhou. 2014. « Effect of GO
856 nanosheets on shapes of cement hydration crystals and their formation process ».
857 *Construction and Building Materials*, vol. 64, p. 231-239.
858 <https://doi.org/10.1016/j.conbuildmat.2014.04.061>.

859 Lv, Shenghua, Yujuan Ma, Chaochao Qiu, Ting Sun, Jingjing Liu et Qingfang Zhou. 2013.
860 « Effect of graphene oxide nanosheets of microstructure and mechanical properties
861 of cement composites ». *Construction and Building Materials*, vol. 49, p. 121-127.
862 <https://doi.org/10.1016/j.conbuildmat.2013.08.022>.

863 Meng, Shaoqiang, Xiaowei Ouyang, Jiyang Fu, Yanfei Niu et Yuwei Ma. 2021. « The role
864 of graphene/graphene oxide in cement hydration ». *Nanotechnology Reviews*, vol.
865 10, n° 1, p. 768-778. <https://doi.org/10.1515/ntrev-2021-0055>.

866 Mirsayapov, Ilshat, Samat Yakupov et Majd Hassoun. 2020. « About concrete and
867 reinforced concrete corrosion ». *IOP Conference Series: Materials Science and*
868 *Engineering*, vol. 890, p. 012061. <https://doi.org/10.1088/1757-
869 899X/890/1/012061>.

870 Mohammed, A., N. T. K. Al-Saadi et J. Sanjayan. 2018. « Inclusion of graphene oxide in
871 cementitious composites: state-of-the-art review ». *Australian Journal of Civil*
872 *Engineering*, vol. 16, n° 2, p. 81-95.
873 <https://doi.org/10.1080/14488353.2018.1450699>.

874 Nkinamubanzi, P.-C., S. Mantellato et R.J. Flatt. 2016. « Superplasticizers in practice ».
875 In *Science and Technology of Concrete Admixtures*, p. 353-377. Elsevier.
876 <https://doi.org/10.1016/B978-0-08-100693-1.00016-3>. Consulté le 7 janvier
877 2022.

878 Scrivener, Karen L., Vanderley M. John et Ellis M. Gartner. 2018. « Eco-efficient cements:
879 Potential economically viable solutions for a low-CO2 cement-based materials
880 industry ». *Cement and Concrete Research*, vol. 114, p. 2-26.
881 <https://doi.org/10.1016/j.cemconres.2018.03.015>.

882 Shang, Yu, Dong Zhang, Chao Yang, Yanyun Liu et Yong Liu. 2015. « Effect of graphene
883 oxide on the rheological properties of cement pastes ». *Construction and Building*
884 *Materials*, vol. 96, p. 20-28. <https://doi.org/10.1016/j.conbuildmat.2015.07.181>.

885 Stanish, K D, R D Hooton et M D A Thomas. 1997. « Testing the Chloride Penetration
886 Resistance of Concrete: A Literature Review ». p. 33.

887 Wang, Juan, Yaoqun Xu, Xiaopeng Wu, Peng Zhang et Shaowei Hu. 2020. « Advances of
888 graphene- and graphene oxide-modified cementitious materials ». *Nanotechnology*
889 *Reviews*, vol. 9, n° 1, p. 465-477. <https://doi.org/10.1515/ntrev-2020-0041>.

890 Yang, Haibin, Manuel Monasterio, Hongzhi Cui et Ningxu Han. 2017. « Experimental
891 study of the effects of graphene oxide on microstructure and properties of cement
892 paste composite ». *Composites Part A: Applied Science and Manufacturing*, vol.
893 102, p. 263-272. <https://doi.org/10.1016/j.compositesa.2017.07.022>.

894 Zhang, Min-Hong, Kritsada Sisomphon, Tze Siong Ng et Dao Jun Sun. 2010. « Effect of
895 superplasticizers on workability retention and initial setting time of cement
896 pastes ». *Construction and Building Materials*, vol. 24, n° 9, p. 1700-1707.
897 <https://doi.org/10.1016/j.conbuildmat.2010.02.021>.

898 Zhao, Li, Xinli Guo, Yuanyuan Liu, Yuhong Zhao, Zhongtao Chen, Yunsheng Zhang,
899 Liping Guo, Xin Shu et Jiaping Liu. 2018. « Hydration kinetics, pore structure, 3D
900 network calcium silicate hydrate, and mechanical behavior of graphene oxide
901 reinforced cement composites ». *Construction and Building Materials*, vol. 190, p.
902 150-163. <https://doi.org/10.1016/j.conbuildmat.2018.09.105>.

903 Zhao, Li, Shengqing Zhu, Hao Wu, Xingchi Zhang, Qingqing Tao, Luguang Song, Yang
904 Song et Xinli Guo. 2020. « Deep research about the mechanisms of graphene oxide
905 (GO) aggregation in alkaline cement pore solution ». *Construction and Building*
906 *Materials*, vol. 247, p. 118446.
907 <https://doi.org/10.1016/j.conbuildmat.2020.118446>.

908 Zunino, Franco et Karen Scrivener. 2019. « The influence of the filler effect on the sulfate
909 requirement of blended cements ». *Cement and Concrete Research*, vol. 126, p.
910 105918. <https://doi.org/10.1016/j.cemconres.2019.105918>.

911

912

Table 1: Chemical analysis of binders

Oxide (%)	**Slag**	**SF**	**GU**
SiO_2	36.3	96.5	20.4
Al_2O_3	10.3	0.5	4.4
Fe_2O_3	0.9	0.45	2.5
CaO	43.4	0.4	63.0
MgO	6.6	0.4	1.7
Na_2O_{eq}	0.5	0.11	0.53
SO_3	0.2	0.08	3.7

Table 2: Chemical analysis of the commercially available graphene oxide

Element	**Percentage (%)**
Carbon	49-56
Hydrogen	1-2
Nitrogen	0-1
Sulfur	2-4
Oxygen	41-51

Table 3: Samples for isothermal calorimetry

# Mix	GU (g)	GGBFS (g)	Water (ml)	W/B	GO (%)	SP	Sonication
GU 0.4	3.5714	-	1.4286	0.40	-	-	No
GU 0.4 GO	3.5714	-	1.1607	0.40	0.03	-	No
GU 0.4 SP	3.5714	-	1.4286	0.40	-	1	No
GU 0.4 GO+	3.5714	-	1.1607	0.40	0.03	-	Yes
GU 0.4 SP-GO	3.5714	-	1.1607	0.40	0.03	1	No
GU 0.4 SP-GO+	3.5714	-	1.1607	0.40	0.03	1	Yes
GUb-S 0.4	2.7332	0.8382	1.4286	0.40	-	-	No
GUb-S 0.4 GO	2.7332	0.8382	1.1607	0.40	0.03	-	No
GUb-S 0.4 SP	2.7332	0.8382	1.4286	0.40	-	1	No
GUb-S 0.4 GO+	2.7332	0.8382	1.4286	0.40	-	-	Yes
GUb-S 0.4 SP-GO	2.7332	0.8382	1.1607	0.40	0.03	1	No
GUb-S 0.4 SP-GO+	2.7332	0.8382	1.1607	0.40	0.03	1	Yes
GUb-SF 0.4	3.2857	0.2857	1.4286	0.40	-	-	No
GUb-SF 0.4 GO	3.2857	0.2857	1.1607	0.40	0.03	-	No
GUb-SF 0.4 SP	3.2857	0.2857	1.4286	0.40	-	1	No
GUb-SF 0.4 GO+	3.2857	0.2857	1.4286	0.40	0.03	-	Yes
GUb-SF 0.4 SP-GO	3.2857	0.2857	1.1607	0.40	0.03	1	No
GUb-SF 0.4 SP-GO+	3.2857	0.2857	1.1607	0.40	0.03	1	Yes
GU 0.35	3.5714	-	1.2500	0.35	-	-	No
GU 0.35 GO	3.5714	-	0.9821	0.35	0.03	-	No
GU 0.35 SP	3.5714	-	1.2500	0.35	-	1	No
GU 0.35 GO+	3.5714	-	0.9821	0.35	0.03	-	Yes
GU 0.35 SP-GO	3.5714	-	0.9821	0.35	0.03	1	No
GU 0.35 SP-GO+	3.5714	-	0.9821	0.35	0.03	1	Yes
GUb-S 0.35	2.7332	0.8382	1.2500	0.35	-	-	No
GUb-S 0.35 GO	2.7332	0.8382	0.9821	0.35	0.03	-	No
GUb-S 0.35 SP	2.7332	0.8382	1.2500	0.35	-	1	No
GUb-S 0.35 GO+	2.7332	0.8382	1.2500	0.35	-	-	Yes
GUb-S 0.35 SP-GO	2.7332	0.8382	0.9821	0.35	0.03	1	No
GUb-S 0.35 SP-GO+	2.7332	0.8382	0.9821	0.35	0.03	1	Yes
GUb-SF 0.35	3.2856	0.2857	1.2500	0.35	-	-	No
GUb-SF 0.35 GO	3.2856	0.2857	0.9821	0.35	0.03	-	No
GUb-SF 0.35 SP	3.2857	0.2857	1.2500	0.35	-	1	No
GUb-SF 0.35 GO+	3.2857	0.2857	0.9821	0.35	0.03	-	Yes
GUb-SF 0.35 SP-GO	3.2857	0.2857	0.9821	0.35	0.03	1	No
GUb-SF 0.35 SP-GO+	3.2857	0.2857	0.9821	0.35	0.03	1	Yes

Table 4: Materials proportions for mortar mixes

Mix	ID	Sand (g)	GU (g)	GGBFS (g)	W/B	GO (ml)	Water (ml)	SP (ml)	Sonication
1	GU	2035	740	-	0.485	0	359	-	-
2	GU-SP	2035	740	-	0.485	0	359	2	-
3	GU-GO	2035	740	-	0.485	55.5	303.5	-	-
4	GU-SP-GO	2035	740	-	0.485	55.5	303.5	2	-
5	GU-GO +	2035	740		0.485	55.5	303.5	-	Yes
6	GU-SP-GO +	2035	740	-	0.485	55.5	303.5	2	Yes
7	GUb-S	2035	518	222	0.485	0	359	-	-
8	GUb-S-SP	2035	518	222	0.485	0	359	2	-
9	GUb-S-GO	2035	518	222	0.485	55.5	303.5	-	-
10	GUb-S-SP-GO	2035	518	222	0.485	55.5	303.5	2	-
11	GUb-S-GO+	2035	518	222	0.485	55.5	303.5	-	Yes
12	GUb-S-SP-GO+	2035	518	222	0.485	55.5	303.5	2	Yes
13	GUb-SF	2035	680.8	59.2	0.485	0	359	4	Yes
14	GUb-SF-SP	2036	680.8	59.2	0.485	0	359	4	-
15	GUb-SF-GO	2037	680.8	59.2	0.485	55.5	303.5	-	-
16	GUb-SF-SP-GO	2038	680.8	59.2	0.485	55.5	303.5	4	-
17	GUb-SF-GO+	2039	680.8	59.2	0.485	55.5	303.5	-	Yes
18	GUb-SF-SP-GO+	2040	680.8	59.2	0.485	55.5	303.5	4	Yes

Table 5: Type V-S. XIII. C-1. and C-XL concrete requirements

Concrete characteristics based on 3101 and CSA standards	Requirements			
	MTMD		CSA	
	V-S	XIII	C-1	C-XL
Compressive stength (MPa)	35 at 28 d	50 at 28 d	35 at 28 d	50 at 56 d
Minimal binder content kg/m^3	365/340	410	-	-
Binder type	GUb-S/SF. GUb-SF	GUb-S/SF. GUb-SF	-	
W/B	0.40	0.34-0.38	< 0.4	< 0.4
Coarse aggregate (mm)	5 - 20	5 - 14	-	-
Air content (%)	6 - 9	5 - 8	5 - 8	5 - 8
Slump (mm)	90 - 150	140 - 200	-	-
Chloride ion penetration (coulombs)	1500	1000	1500	1000

Table 6: Mix design factors and their levels.

	Factor			
Level	**Binder**	**W/B**	**Superplasticizer**	**Graphene oxide**
1	GU	0.35	Yes	No
2	GUb-S	0.45	No	Yes
3	GUb-SF	-	-	Yes + sonication

Table 7: ANOVA results for the heat released after 160h.

Factor	DF	Sum of Squares	Mean Square	F Value	p-value
Binder	2	1223.4	611.7	83.0	9.98E-13
W/B	1	2846.8	2846.8	386.3	2.63E-18
Superplasticizer	1	63.3	63.3	8.6	0.0065
Graphene oxide	2	13.3	6.6	0.9	0.4174
Error	29	213.7	7.4		
Total	35	4360.6			

Table 8: ANOVA results for the mortar compressive strength.

	Factor		
Level	**Binder**	**Superplasticizer**	**Graphene oxide**
1	GU	Yes	No
2	GUb-S	No	Yes
3	GUb-SF	-	Yes + sonication

Table 9: ANOVA results for the mortar compressive strength at 1 day.

Factor	**DF**	**Sum of Squares**	**Mean Square**	**F Value**	**p-value**
Binder	2	173.4	86.7	31.7	1.63E-05
Superplasticizer	1	19.3	19.3	7.1	0.0211
Graphene_oxide	2	4.32	2.2	0.79	0.4762
Error	12	32.9	2.7		
Total	17	229.9			

Table 10: ANOVA results for the mortar compressive strength at 28 days.

Factor	**DF**	**Sum of Squares**	**Mean Square**	**F Value**	**p-value**
Binder	2	81.9	40.9	8.6	0.0045
Superplasticizer	1	406.5	406.5	86.9	7.60E-07
Graphene_oxide	2	71.4	35.7	7.6	0.0073
Error	12	56.1	4.7		
Total	17	615.9			

Table 11: Fresh and hardened characteristics of concrete

Properties / Mixes		Air content %	Slump mm	Density kg/m^3	Compressive strength (28d) MPa
TYPE V-S	**GU 0.4**	10.0	115	2263	37.2 ± 2.8
	GU-GO 0.4	7.9	100	2314	40.8 ± 0.9
	GUb-30S 0.4	9.0	115	2280	38.5 ± 4.4
	GUb-30S+GO 0.4	7.5	100	2343	45.0 ± 2.4
	GUb-S/SF 0.4	10.0	120	2255	38.3 ± 5.4
TYPE XIII	**GU 0.35**	8.0	190	2321	56.8 ± 1.3
	GU+GO 0.35	6.7	155	2339	57.9 ± 1.0
	GUb-30S 0.35	5.0	190	2390	65.0 ± 2.1
	GUb-30s+GO 0.35	8.0	200	2327	61.0 ± 1.0
	GUb-S/SF 0.35	6.8	170	2362	60.0 ± 0.4

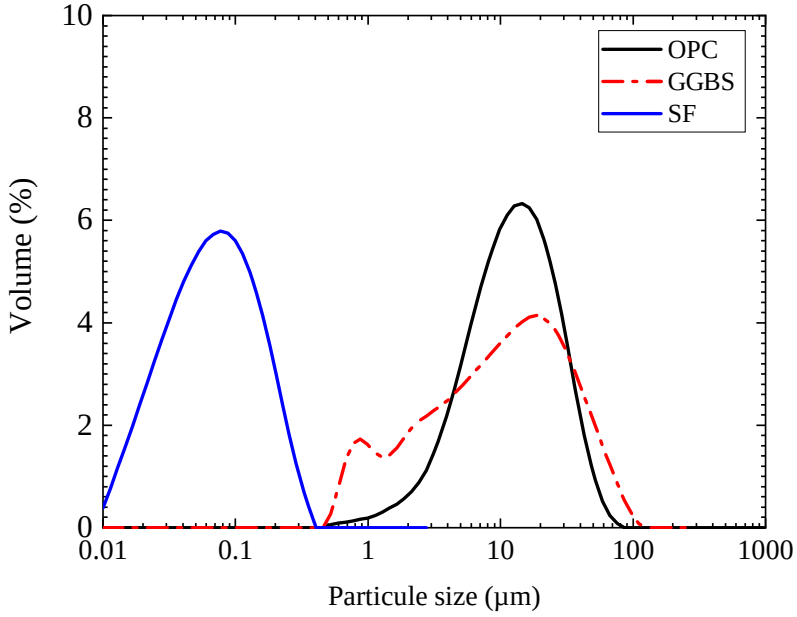

Figure 1: Particle size distribution of binders

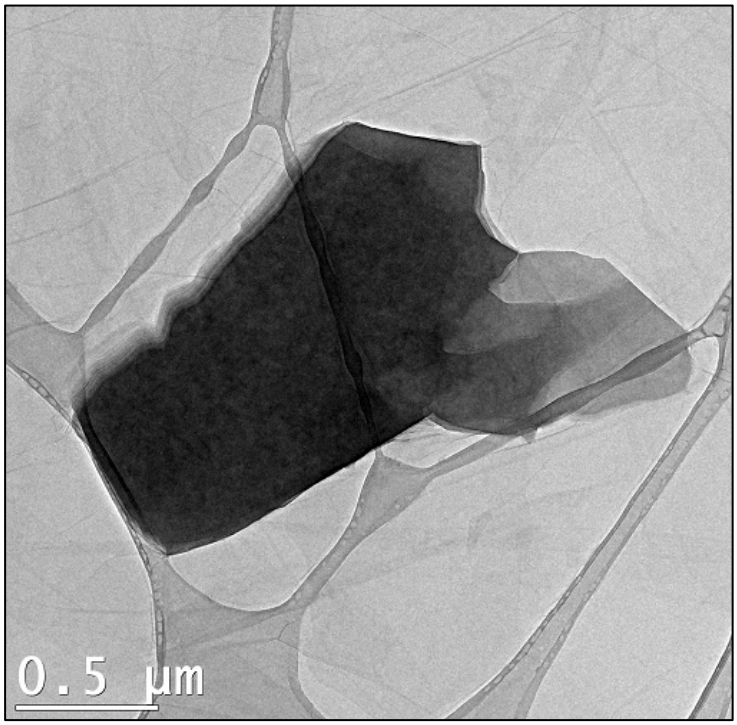

Figure 2: GO particle under TEM.

Credit: Thomas Duplessis

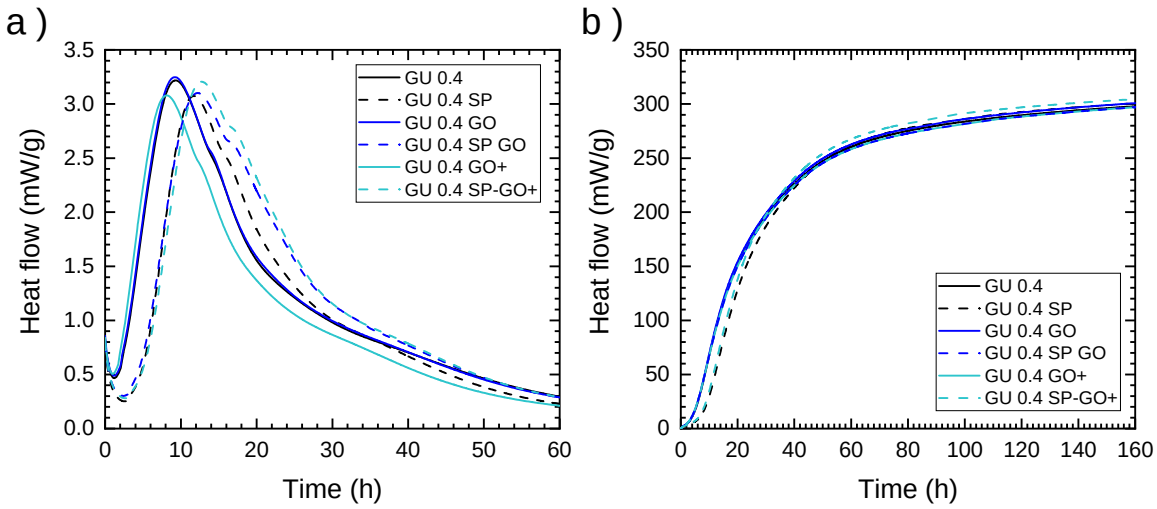

Figure 3: a) Heat flow (mW/g) vs. time and b) cumulative heat (J/g) vs. time for GU mixes with 0.4 W/B ratio.

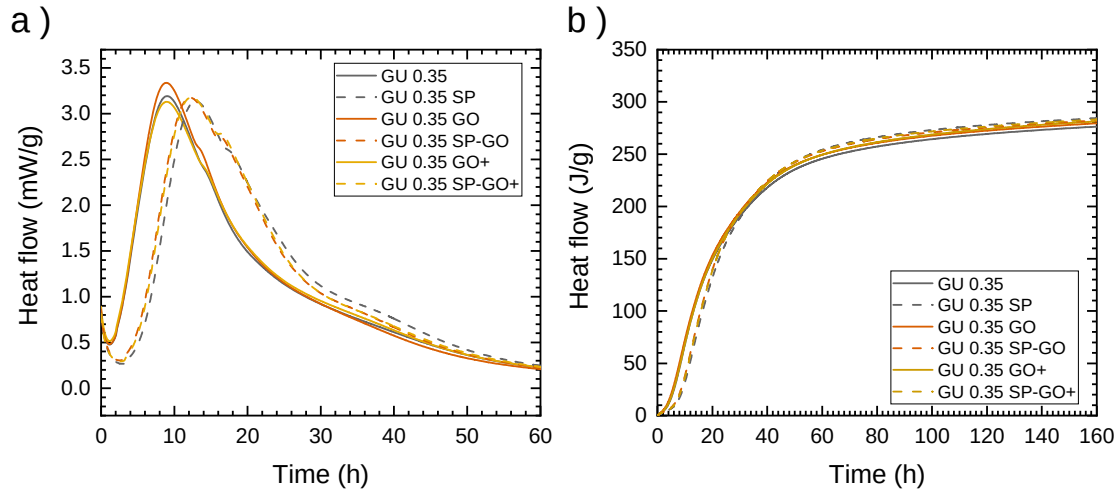

Figure 4: a) Heat flow (mW/g) vs. time and b) cumulative heat (J/g) vs. time for GU mixes with 0.35 W/B ratio

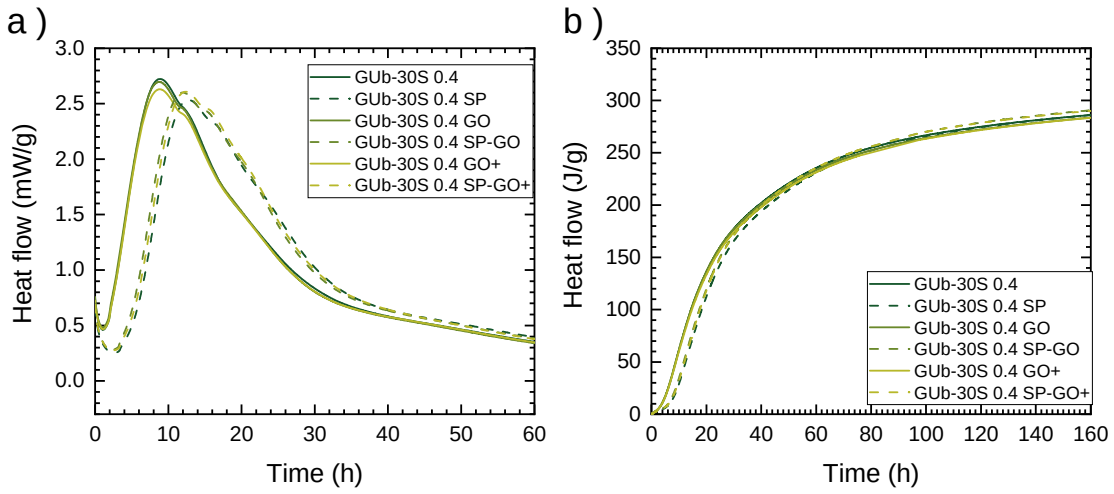

Figure 5: a) Heat flow (mW/g) vs. time and b) cumulative heat (J/g) vs. time for GUb-S mixes with 0.4 W/B ratio.

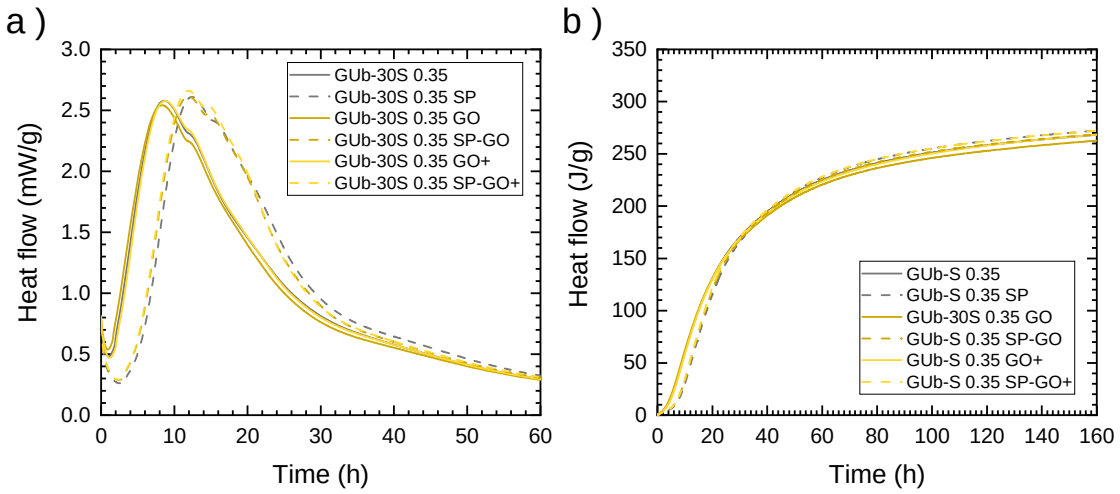

Figure 6: a) Heat flow (mW/g) vs. time and b) cumulative heat (J/g) vs. time for GUb-S mixes with 0.35 W/B ratio.

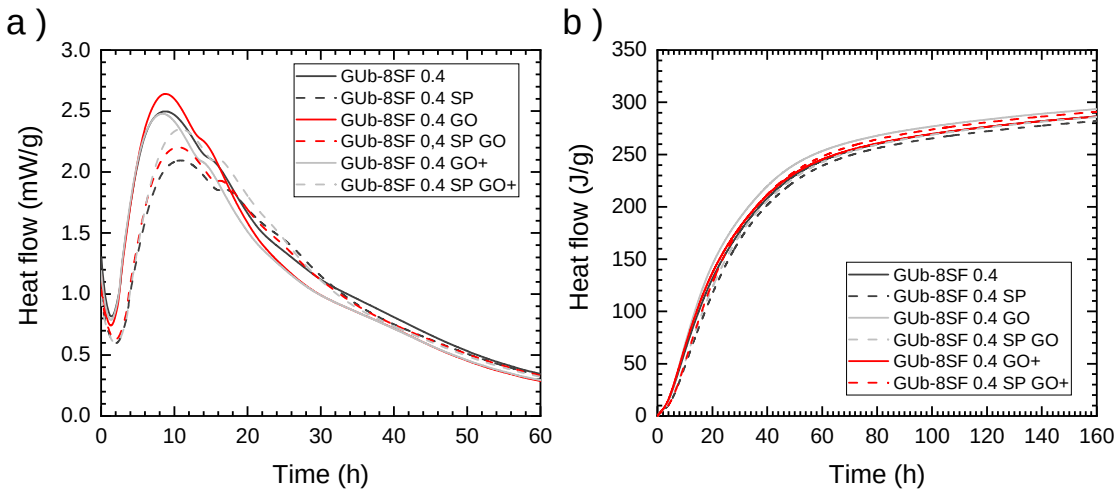

Figure 7: a) Heat flow (mW/g) vs. time and b) cumulative heat (J/g) vs. time for GUb-SF mixes with 0.4 W/B ratio.

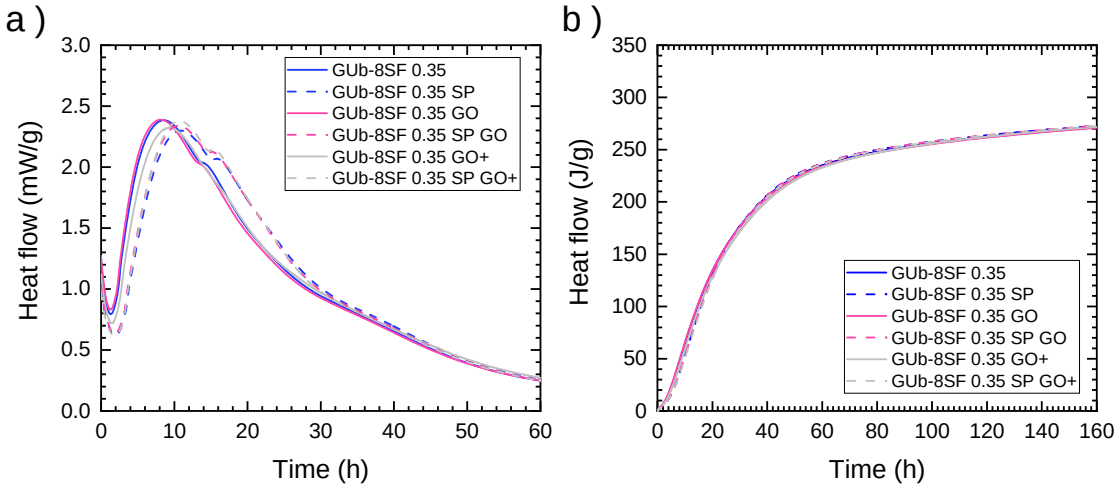

Figure 8: a) Heat flow (mW/g) vs. time and b) cumulative heat (J/g) vs. time for GUb-SF mixes with 0.35 W/B ratio.

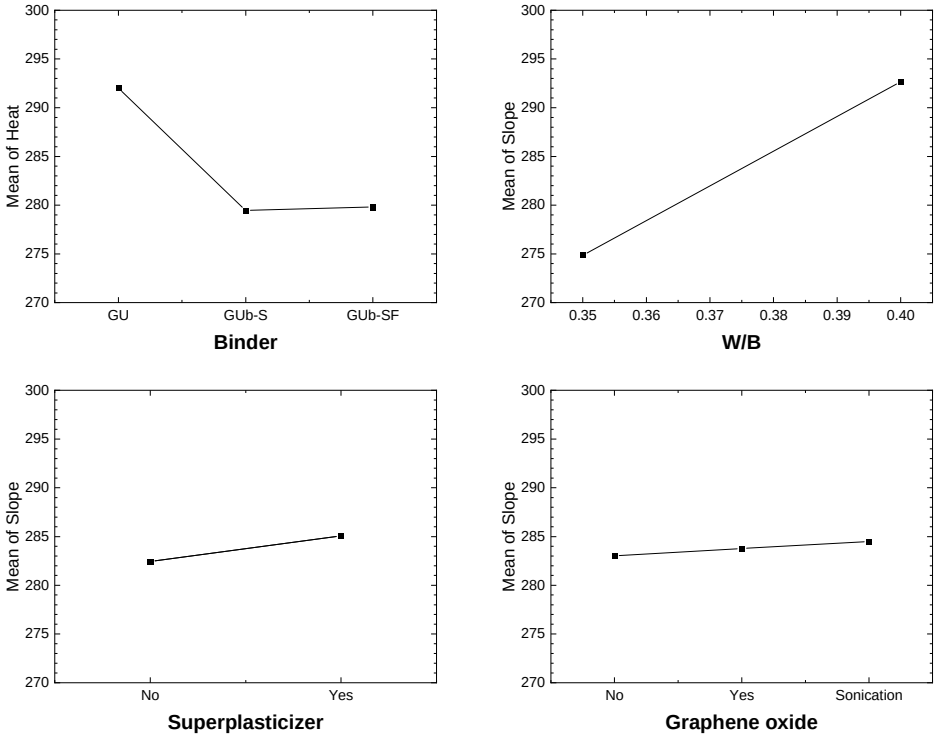

Figure 9: Mean effects plot for the heat released after 160h.

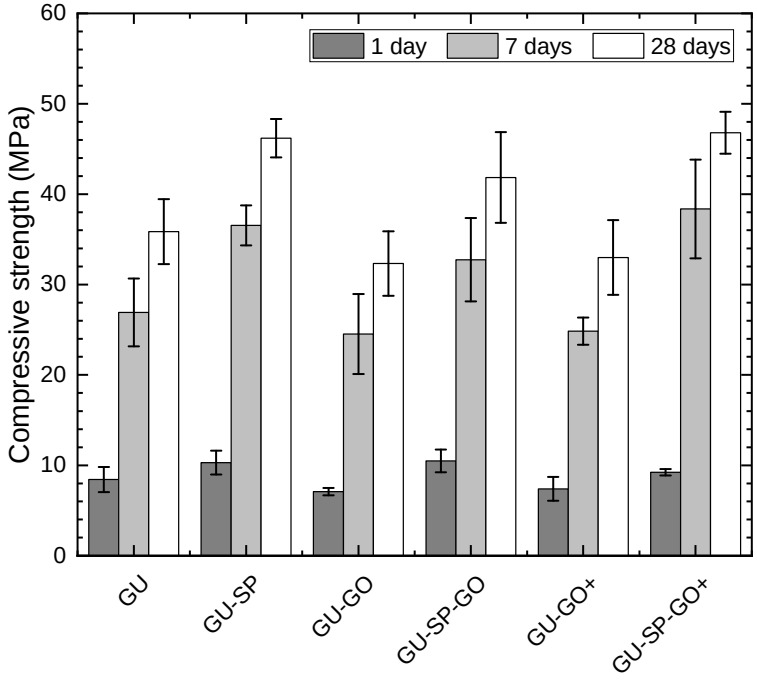

Figure 10: Compressive strength for GU mortars at 1, 7 et 28 days

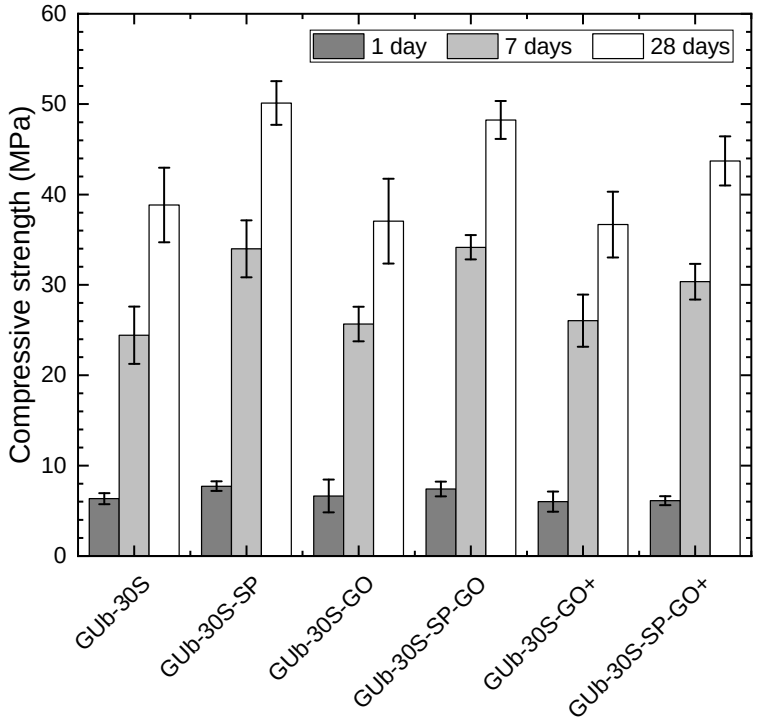

Figure 11 Compressive strength for GUb-S mortars at 1, 7, and 28 days

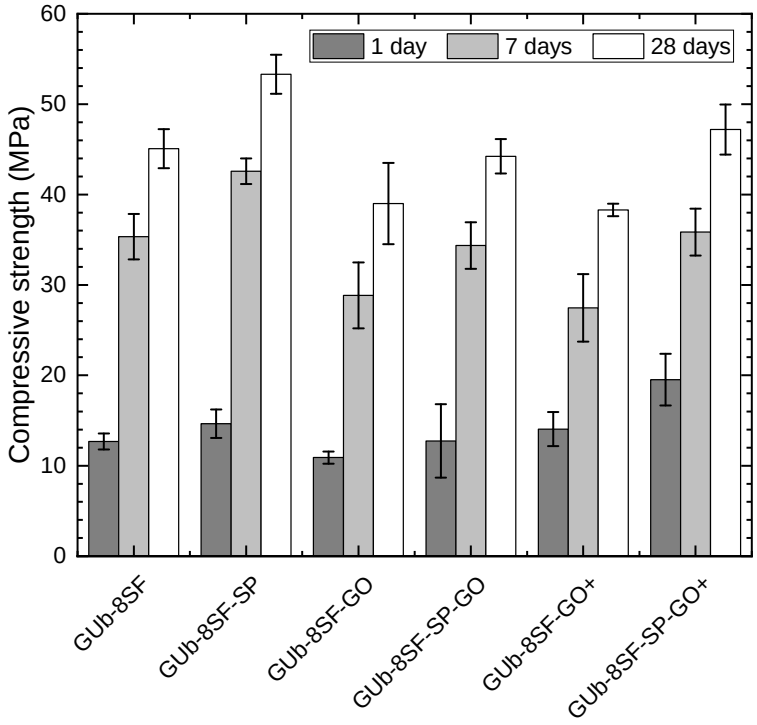

Figure 12 Compressive strength for GUb-SF mortars at 1, 7 et 28 days

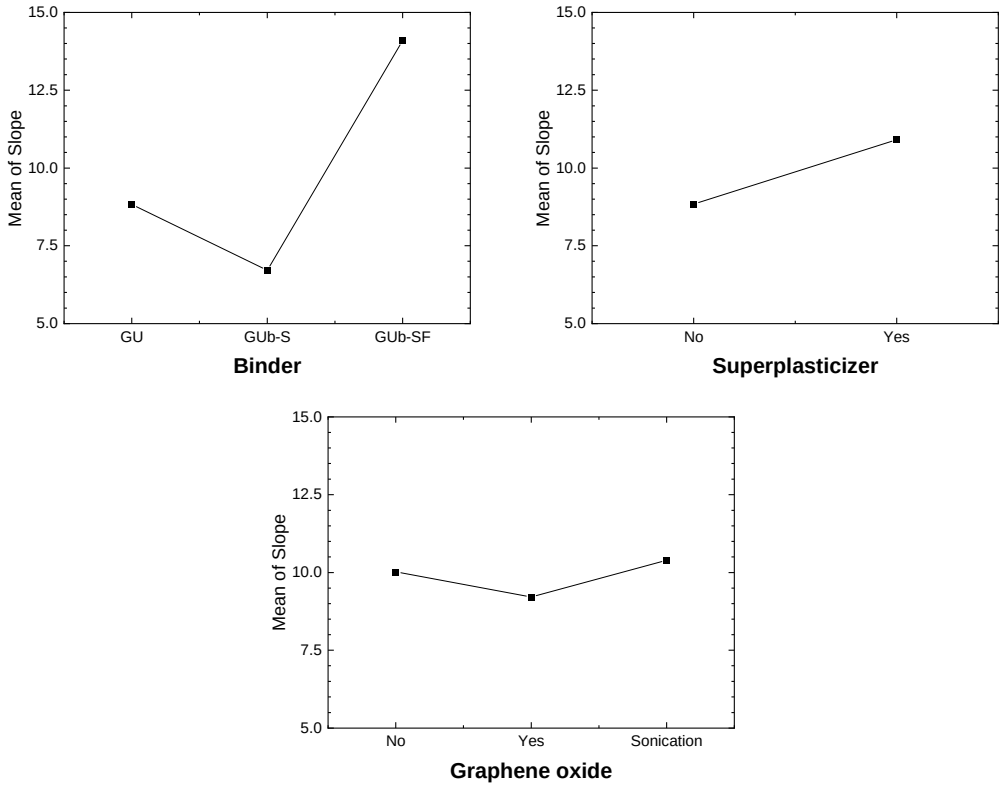

Figure 13: Mean effects plot for the mortar compressive strength at 1 day.

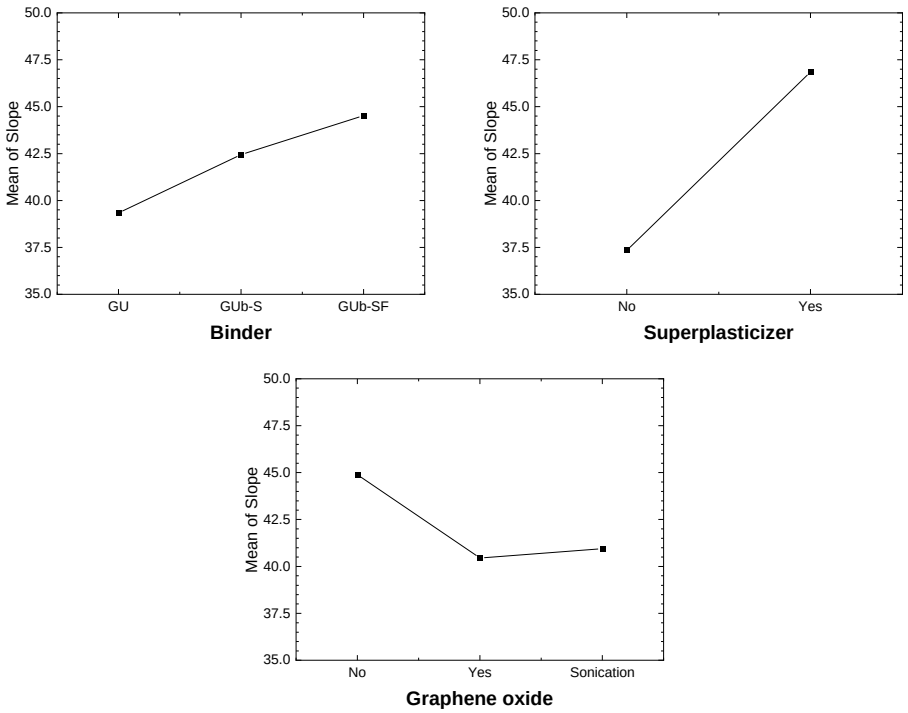

Figure 14: Mean effects plot for the mortar compressive strength at 28 days.

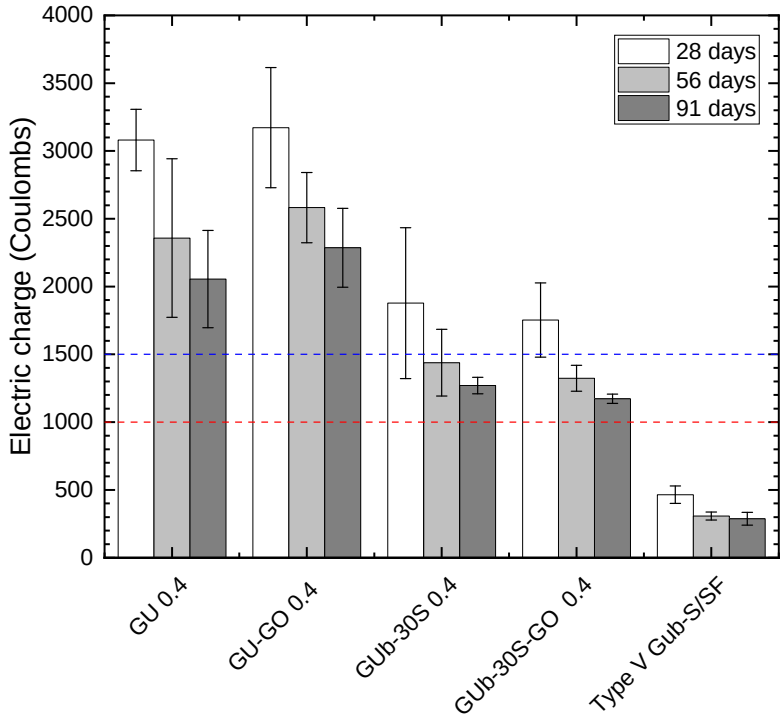

Figure 15: RCPT results for type V-S/C-1 mixes (the red line shows the standard required and the mixes below the line are acceptable)

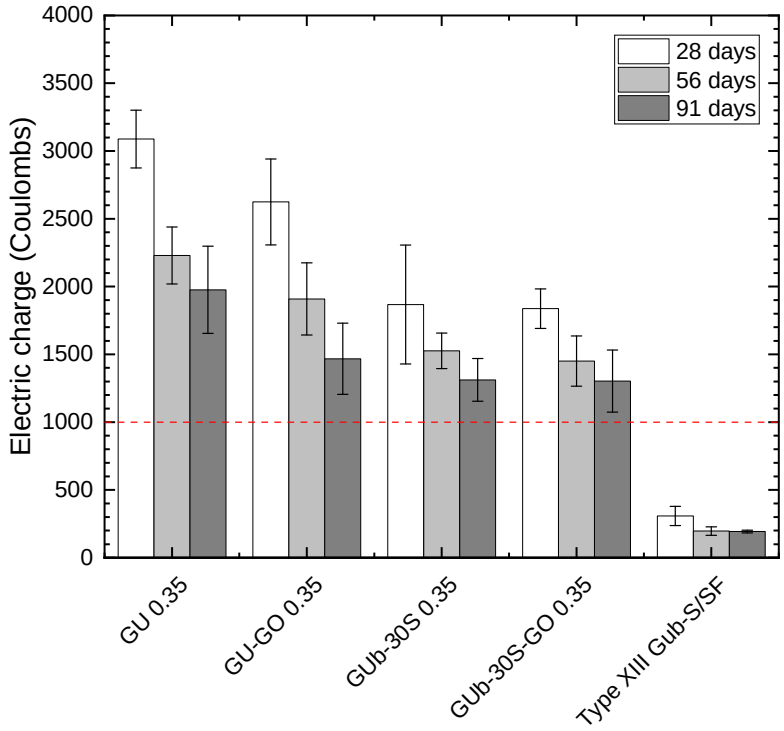

Figure 16: RCPT results for type XIII/C-XL mixes (the red line shows the standard required and the mixes below the line are acceptable)